Supplemental Material

Drug Metabolism and Disposition

Plasma and liver protein binding of GalNAc conjugated siRNA

Sara. C. Humphreys[1*], Mai B. Thayer[1], Julie M. Lade[1], Bin Wu[2], Kelvin Sham[2], Babak Basiri[1], Yue Hao[3], Xin Huang[3], Richard Smith[1] and Brooke M. Rock[1]

[1]Pharmacokinetics and Drug Metabolism Department, Amgen Research, 1120 Veterans Boulevard, South San Francisco, CA, 94080, USA

[2]Hybrid Modality Engineering Department, Amgen Research, One Amgen Center Drive, Thousand Oaks, CA, 91320, USA

[3]Molecular Engineering Department, Amgen Research, 360 Binney Street, Cambridge, MA, 02141, USA

*Corresponding author

Supplemental Methods

Recovery of siRNA-X in PBST by 20 MWCO equilibrium dialysis

Device Preparation: Pre-soak Slide-A-Lyzer 20 kDa MWCO equilibrium dialysis units in a large volume of PBST for 2 hours, then replace the buffer and leave overnight. Immediately prior to use, pick up device with tweezers and tap vigorously to remove excess liquid.

Sample Preparation: Add 100 µL siRNA-X spiked in PBST to each device. Place in receiver chamber containing 1.8 mL PBST and leave to equilibrate overnight at 37°C, shaking at 500 rpm. Once at equilibrium, remove device, thoroughly mix sample in receiver.

siRNA Detection and Quantitation: By hybridization ELISA (see main body).

Results: ultrafiltration siRNA-X recovery in buffer is reported in Table 1.

Recovery of siRNA-X in PBST by ultracentrifugation

Sample Preparation: siRNA working stocks were prepared in 1x PBS and added to PBST buffer for a final concentration of 1 µM. Following an equilibration for 15 min at 37°C, each sample (200 µL) was transferred to polycarbonate tubes (7 x 20 mm) in triplicate and centrifuged at 390,880 *x*g for 3 hours at 37°C using an Optima TLX Ultracentrifuge (Beckman Coulter). After centrifugation, 50 µL of supernatant (3 h) was removed for recovery analysis.

siRNA Detection and Quantitation: Samples were diluted 1:10 in hybridization ELISA sample buffer for siRNA quantitation. The final recovered fraction was calculated using the following equation:

$$Unbound\ fraction = \frac{Ultracentrifuge\ supernatant\ at\ 3\ h}{Spiked\ buffer\ at\ 0\ h}$$

Results: Ultracentrifugation siRNA-X recovery in buffer experiments are reported in Table 1.

Recovery of siRNA-X, siRNA-Y and siRNA-Z in PBS+CHAPS by ultrafiltration

To compare 50 MWCO ultrafiltration recovery using PBST and PBS+CHAPS (0.1% (w/v) CHAPS), we repeated the recovery experiment described in the Methods section, replacing PBST with PBS+CHAPS for filter pre-treatment and for siRNA spikes (1 µM siRNA-X, siRNA-Y and siRNA-Z; structural topology of each of these molecules is depicted in Supplemental Figure 3).

Small molecule $f_{u,plasma}$ *and* $f_{u,liver}$ ultracentrifugation method

Neat pooled and mixed gender human plasma was titrated to a pH of 7.2-7.4. Antipyrine and timolol working stocks were prepared in 1x PBS and added to plasma for a final concentration of 1.0 µM. Rosuvastatin was similarly prepared in liver homogenate. Following equilibration for 15 minutes at 37°C, each suspension (200 µL) was transferred to polycarbonate tubes (7 × 20 mm) in triplicate and centrifuged at 390,880 *x*g for 3 h at 37°C using an Optima TLX Ultracentrifuge (Beckman Coulter). To facilitate the calculation of fraction unbound, 50 µL of initial spiked plasma suspensions (0 hour) were added in triplicate to 50µL plasma ultrafiltrate for each respective species. After centrifugation, 50 µL of supernatant (3 hours) was removed and added to plasma ultrafiltrate. Samples were diluted 1:10 in hybridization-ligation sample buffer for siRNA quantitation via LC-MS/MS. The final plasma unbound fraction was calculated by dividing the small molecule signal in the ultracentrifuge supernatant by the spiked plasma at 0 hours. Results are reported in Table 2.

EMSA of siRNA-plasma 50 MWCO ultrafiltrate

Part I: EMSA to investigate siRNA-protein binding in the ultrafiltrate

Sample preparation: Add 4 µL ultrafiltrate (receiver compartment) or spiked plasma (donor compartment) to 20 µL 1× sample buffer (Novex Hi-Density TBE Sample Buffer (Thermo Fisher, #LC6678)), load 5 µL onto a 20% PAGE gel and run at 200 V. Stain with SYBR Gold according to the manufacturer's instructions (Thermo Fisher, #S11494) and image using UV transillumination.

Data analysis: Visual comparison

Results: Supplemental Figure 2A shows two major SYBR Gold-staining bands in the plasma ultrafiltrate and one band in the buffer control ultrafiltrate. For each siRNA construct, the lower band in the plasma ultrafiltrate corresponds to the band in the buffer control, indicating "unbound" siRNA. We suspected that the upper band corresponded to albumin, which was confirmed in the Supplemental Figure 2B. In Figure S5, we show that albumin does not bind to siRNA-X up to 1 µM, therefore, Supplemental Figure 2A demonstrates that the vast majority of siRNA in the ultrafiltrate is unbound.

PART II: Electrophoretic Mobility Shift Assay to query whether the additional band observed in plasma was associated with albumin

Sample preparation: Perform a 1:1 titration of albumin binding protein (~22 kDa, generated in-house) into 10% human plasma (12 pt + blank; top concentration: 164 µM) in TBE and incubate for 30 min. at 30° C. Load, run, stain and visualize gel as above.

*Results***:** Supplemental Figure 3B shows that a known albumin binding protein (an engineered version of Protein G) was able to displace the putative albumin band in human plasma, thus confirming its identity. Note that in this experiment, no siRNA was present, so albumin itself stains with SYBR Gold, perhaps as the result of some endogenous nucleotide binding. The albumin binding protein did not stain with SYBR Gold (data not shown). The observation that some fraction of albumin gets through the 50 kDa MWCO filter is not too surprising given the high abundance of albumin and plasma and the fact that the 50 kDa MWCO exclusion limit actually represents a distribution of filter pore sizes.

BLI of various siRNA-like constructs to inform understanding of orientation and GalNAc effects in human and rat plasma

Sample Preparation: As for time-to-equilibrium experiments described in Methods section with the exception that a panel of biotinylated siRNA-like constructs were used. The panel included, the anti-sense or the sense strand of siRNA-X hybridized with a complementary fully 2′OMe sequence that was conjugated with biotin at either the 5′ or the 3′ terminus. In addition, we loaded the single-stranded biotinylated fully 2′OMe strands alone. We used rat plasma in addition to human plasma at the same concentrations.

Results: This panel highlighted the effects of orientation, GalNAc conjugation, ds vs. ssRNA, sequence differences, and chemical modification differences (siRNA-X sense and antisense do not have the same chemical modification patterns or composition).

LC-MS analysis: 1.0 µM siRNA was added to 200 µL aliquots of rat plasma either at the beginning or at the end of a 48 hr incubation period at 37°C. Extraction of siRNA from samples was accomplished by utilizing Clarity OTX SPE plates (Phenomenex, Torrance, CA). The LC-MS analysis was performed using an Agilent Technologies (Santa Clara, CA) 1290 Infinity series UPLC system consisting of a binary pump, a refrigerated autosampler and a temperature-controlled column compartment (TCC) coupled to a Thermo Scientific (Waltham, MA) Q Exactive HF-X Orbitrap mass spectrometer. Samples were separated on a Waters (Milford, MA) 2.1 X 50 mm Acquity UPLC Oligonucleotide BEH C18 Column (130 Å, 1.7 µm) at 80°C. Mobile phase A consisted of 15 mM triethylamine (TEA), 400 mM hexafluoroisopropanol (HFIP) in water and mobile phase B was 15 mM TEA, 400 mM HFIP in methanol. 20 µL of each sample was injected at a 0.4 mL/min flow rate under the following gradient condition (min – %B): 0 – 2 , 1.5 – 2 , 11.5 – 60 , 12 – 95 , 14 – 95 , 14.5 – 2 , 15.5 – 2. The total runtime was 16 minutes and the LC output was diverted to waste from 0 – 2 min and 12 – 16 min.

The mass spectrometer was operated with the following parameters: spray voltage (3.2 kV), capillary temperature (320°C), sheath gas flow rate (50 arbitrary units), sweep gas flow rate (1 arbitrary units), auxillary gas flow rate (10 arbitrary units), auxillary gas temperature (425°C), Full scan negative-ion mode with 60,000 resolution. Instrument control and data acquisition was performed using the Xcalibur 4.0 from Thermo Scientific (Waltham, MA). Corresponding extracted ion chromatograms (XICs) were examined for the expected m/z of sense and antisense strands to determine their stability in plasma.

Supplemental Figures

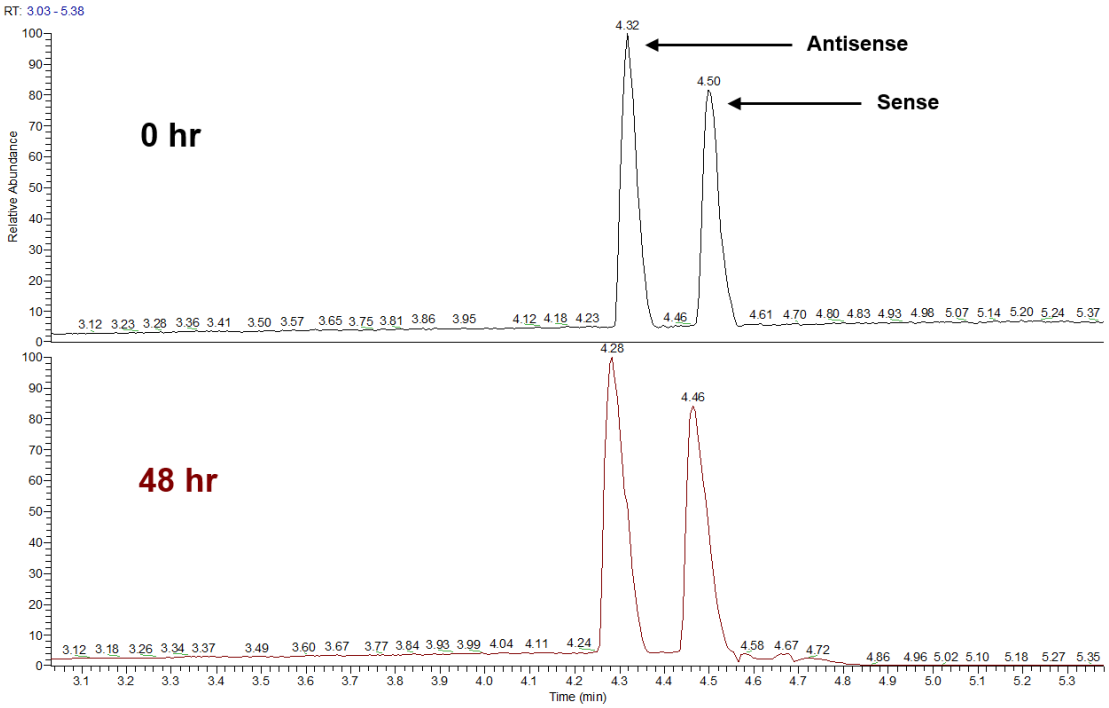

Supplemental Figure 1: Rat plasma stability data of siRNA-X.

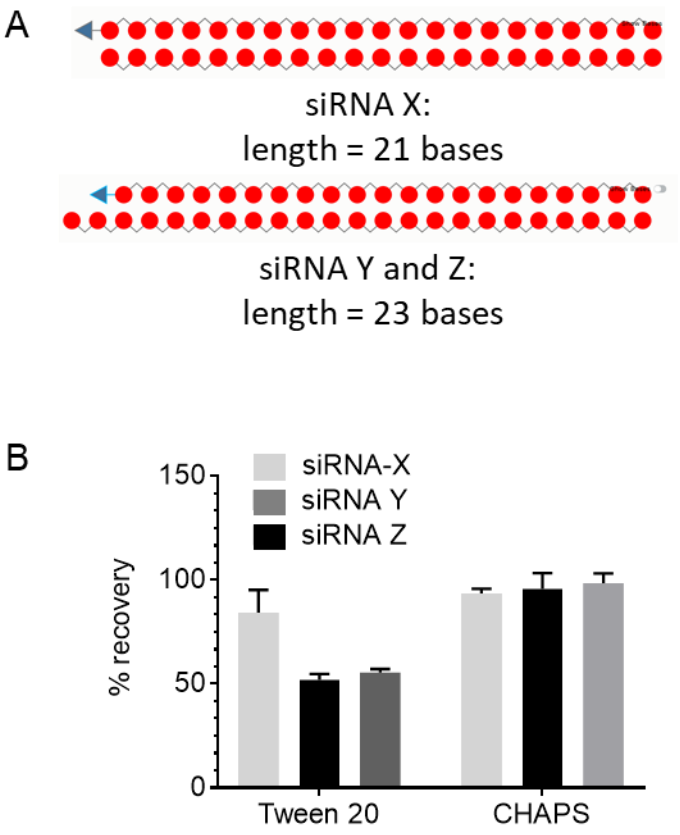

Supplemental Figure 2: The effect of siRNA length and detergent on recovery in buffer via 50 MWCO ultrafiltration. (A) Topographical structural depictions of siRNA-X, siRNA-Y and siRNA-Z. Triantennary GalNAc is depicted as a blue triangle. siRNA-X is a bluntmer containing 2'OMe, 2'F and PS modifications. siRNA-Y and siRNA-Z are asymmetric and contain 2'OMe, 2'F and PS modifications. (B) Recovery in in filters pre-treated with PBST (0.5% Tween-20) or PBS-CHAPS (0.1% CHAPS).

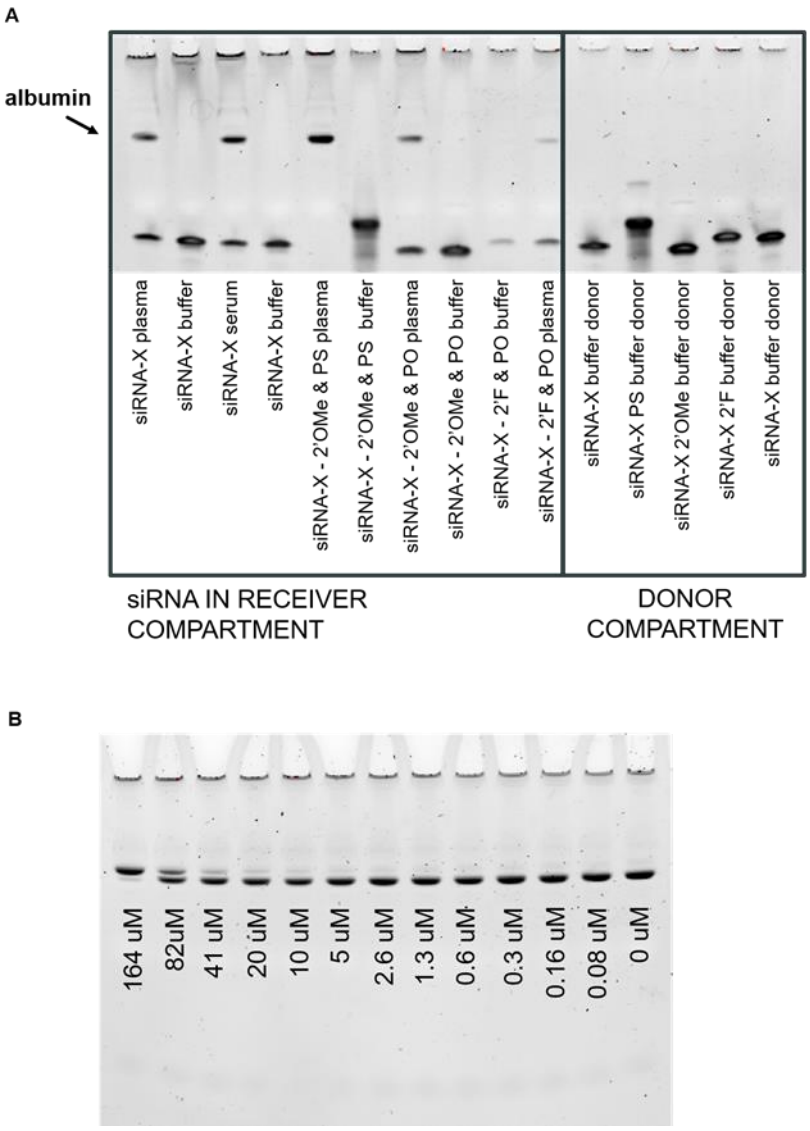

Supplemental Figure 3: The majority of siRNA in the plasma ultrafiltrate after 50 MWCO ultrafiltration is unbound by EMSA. (A) Shows side-by-side plasma and buffer ultrafiltrate recovery of the various siRNA-X constructs shown in Figure 4A. The relative band intensities visually reflect the PPB values reported in Figure 4B. (B) Shows that the upper band in (A) stains with SYBR Gold in the absence of siRNA, and that the band can be displaced with an albumin binding protein.

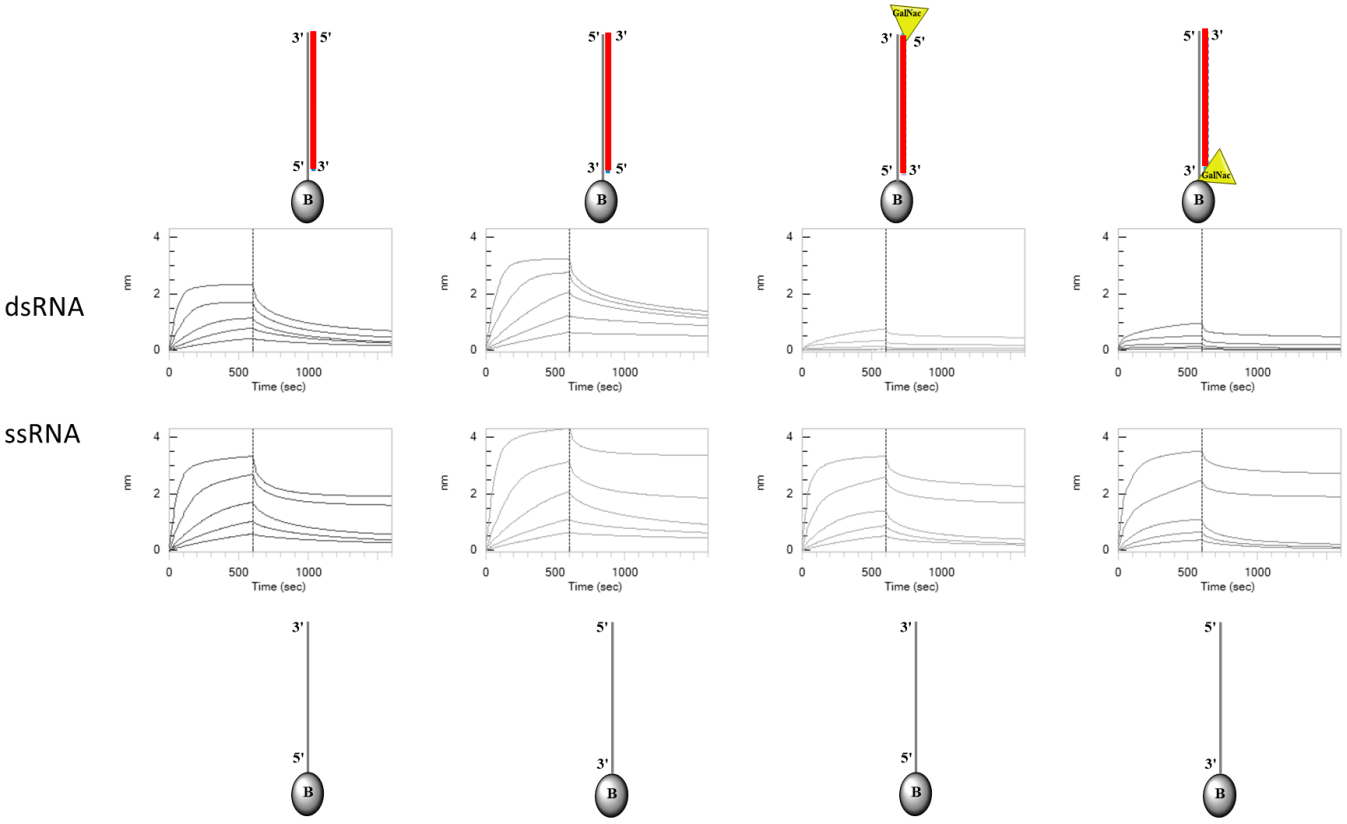

Supplemental Figure 4: Binding of a panel of biotinylated siRNA-X related constructs to a titration of human plasma. TOP ROW: dsRNA constructs with the sense or antisense strand of siRNA-X (colored) hybridized to a biotinylated fully 2'OMe complementary strand. All four possible combinations and orientations loaded as depicted. The yellow triangle represents the GalNAc position when the siRNA-X sense strand is present. BOTTOM ROW: ssRNA versions of what was run on the top row, with "sense-like" 2'OMe sequences on the left and "antisense-like" 2'OMe sequences on the right.

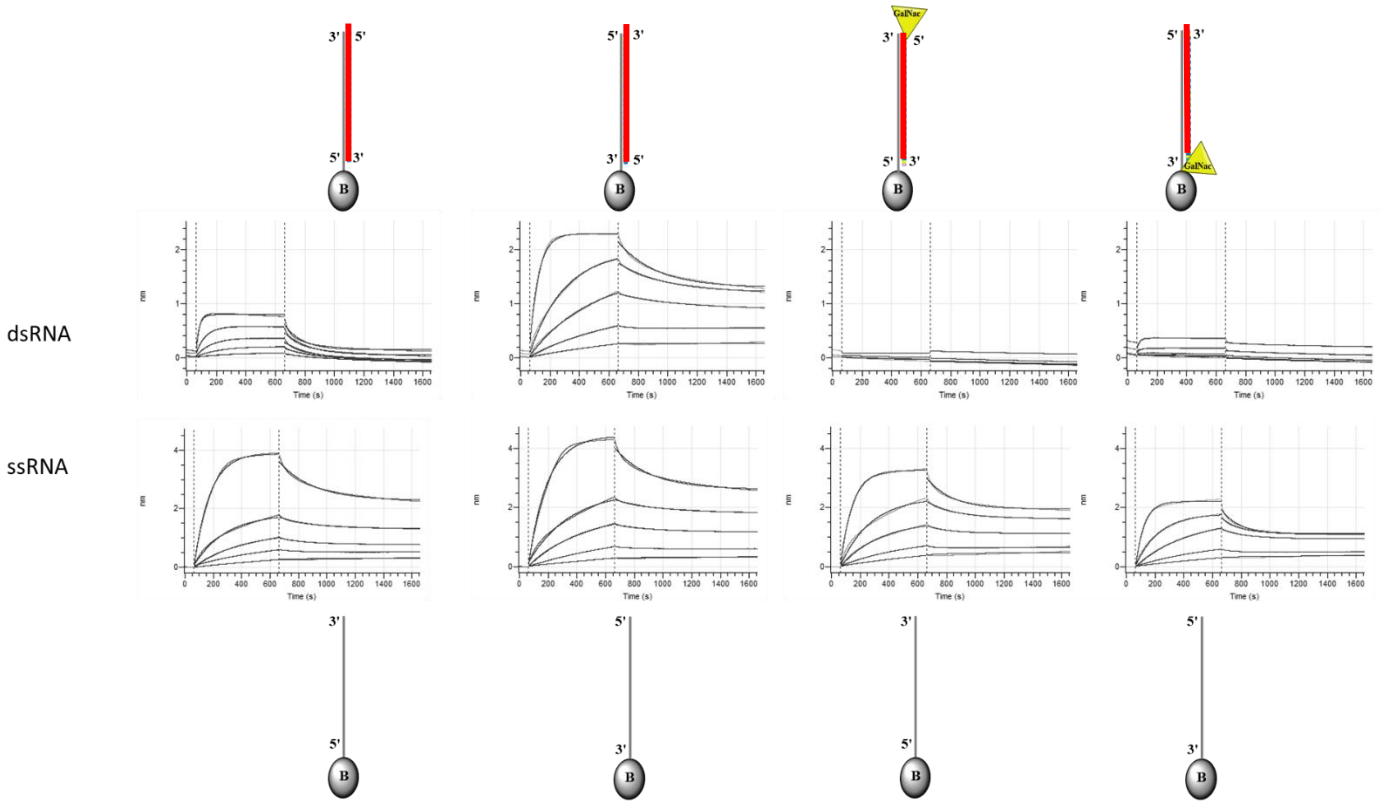

Supplemental Figure 5: Binding of a panel of biotinylated siRNA-X related constructs to a titration of rat plasma. TOP ROW: dsRNA constructs with the sense or antisense strand of siRNA-X (colored) hybridized to a biotinylated fully 2'OMe complementary strand. All four possible combinations and orientations loaded as depicted. The yellow triangle represents the GalNAc position when the siRNA-X sense strand is present. BOTTOM ROW: ssRNA versions of what was run on the top row, with "sense-like" 2'OMe sequences on the left and "antisense-like" 2'OMe sequences on the right.

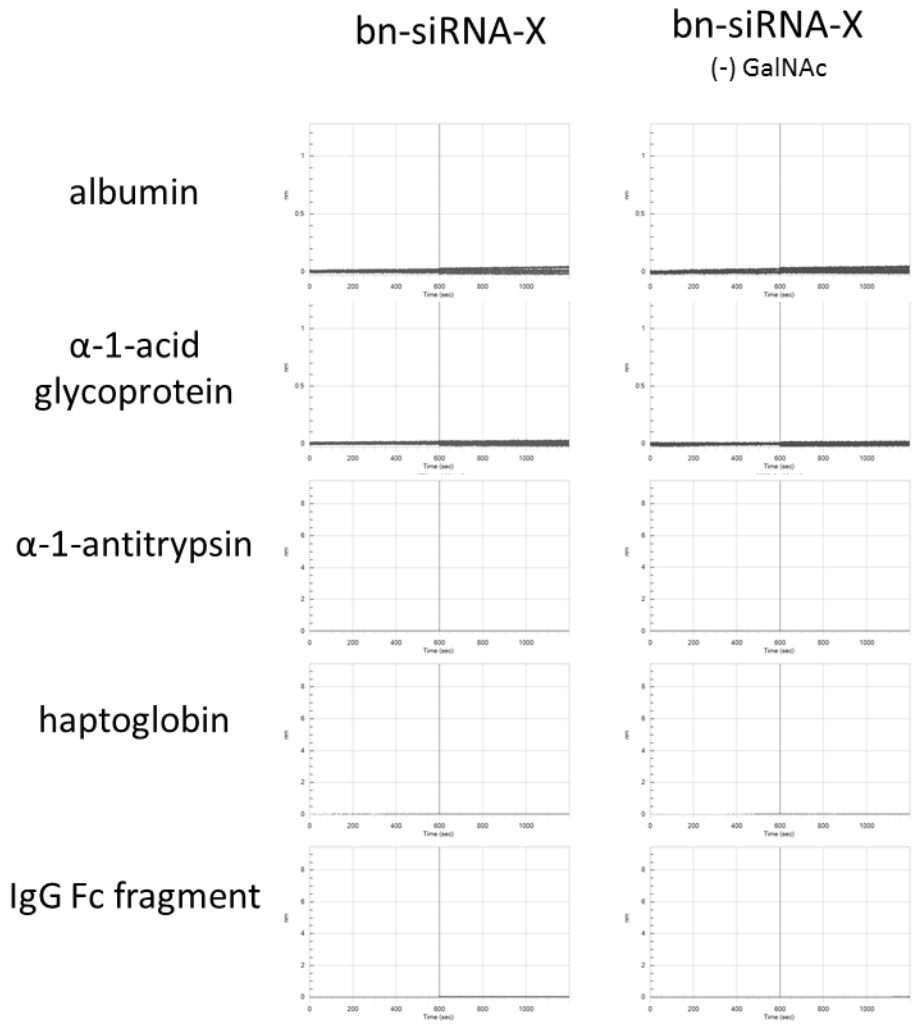

Supplemental Figure 6: negative results of BLI experiment shown in Figure 5. At concentrations up to 1 µM, the following human plasma proteins do not bind to bn-siRNA-X ± GalNAc: albumin, α-1-acid glycoprotein, α-1-antitrypsin, haptoglobin and IgG Fc.

Supplemental Calculation 1: Example R_h calculation

Angstroms per dsRNA helix base-pair (from literature):	2.77 Å/bp
Convert to nanometers:	0.277 nm/bp
Typical number of base-pairs in siRNA:	21
Total length of siRNA:	21 × 0.277 = 5.817 nm
R_h	5.817 nm / 2 = 2.910 nm

Supplemental Calculation 2: M_w (in kDa) estimation for a protein with an equivalent R_h to siRNA

Line equation from linear regression fit of M_w vs R_h (Figure 6)	y = 0.03509x + 1.233
Fix y at 2.910 nm and solve for x	x = (2.910 – 1.233) / 0.03509
	x = 47.8 kDa

Supplemental Discussion

Interpretation of specific siRNA-plasma protein binding interactions

The negative finding for albumin and α1-acid glycoprotein is consistent with a report that less than 2.1% of patisiran, the first and only current FDA-approved siRNA, is bound to these proteins in vitro, however details of the method have not been provided (ONPATTRO™ [patisiran] HIGHLIGHTS OF PRESCRIBING INFORMATION 2018, found at https://www.alnylam.com/wp-content/uploads/2018/08/ONPATTRO-Prescribing-Information.pdf on December 4, 2018). The fact that fibrinogen and fibronectin did not bind to bn-siRNA-X, suggests that these proteins do not bind to GalNAc, and that in this assay format, GalNAc blocks siRNA-X binding. Interestingly, although less siRNA-X protein binding was observed in serum vs. plasma, the difference was not statistically significant, indicating that clotting factors, such as fibrinogen, do not account for a significant proportion of the overall binding observed (Fig. 4).

Given the high concentration of albumin in plasma and serum (530-750 μM (Rustad et al. 2004), it was important for us to understand whether albumin bound to siRNA-X. Our BLI screening assay showed no binding up to 1 μM, meaning that if there is any binding at all, the dissociation constant (K_D), is much greater than 1 μM, and consequently weak, non-specific, and highly transient. We attempted to run this screen at higher concentrations but observed significant solvent-like effects. From the available literature, our finding is consistent with Onishi et al., who found that fully phosphorothioated DNA and locked nucleic acid (LNA) ASOs did not bind to albumin without conjugation to lipophilic ligands using surface plasmon resonance (Onishi et al. 2015); however, it is inconsistent with other groups who showed weak (μM) albumin-ASO interactions with fully phosphorothioated ASOs (Watanabe et al. 2006, Gaus et al. 2018). While these ASO data are potentially informative, again, it is important to remember that ASOs (ssDNA) and siRNA (dsRNA) have very different physicochemical properties and modification patterns likely leading to significant differences in protein binding.

Aside from the pAb, all observed siRNA-protein interactions were highly atypical in that they were multi-phasic and could therefore not be fit to 1:1 binding models. As such, we elected to use the data as a qualitative screen only – assigning sensorgrams as binding "hits" or not. Such screens may be applied in future as a hit-pick based identification of specific siRNA-protein interactions that warrant further investigation. Given the binding complexities observed, we did not attempt to interpret the BLI signal amplitudes for this work. In addition, in performing related studies, we observed significant orientation, strand (double- vs. single-strand), chemical modification type, chemical modification pattern, species, and GalNAc-related orientation effects; all altering the apparent binding affinity of immobilized RNA to plasma proteins (some example sensorgrams provided in Supplemental Figures 4 and 5). This led us to conclude that while surface-based technologies such as BLI provide qualitative insight into whether a protein can bind to RNA, the kinetic data obtained is highly dependent on the method of siRNA immobilization used. To minimize sensorgram complexity, buffer optimization (i.e. changing the pH or salt concentration) may aid to empirically identify more canonical 1:1 binding curves for specific siRNA-protein interactions on a case-by-case basis, however, we advise caution with this approach given that RNA-protein interactions are known to fall along a spectrum ranging from specific to non-specific, and slight buffer alterations could have drastic effects on the apparent affinity and/or number of binding modes (Jankowsky et al. 2015, Gaus et al. 2018). Consequently, the SM- and protein-protein interaction paradigm of globally fitting surfaced-based titrations to 1:1 binding models does not apply to a majority of protein interactions with oligonucleotides such as siRNA.

Finally, although by nature pAbs are heterogenous mixtures – meaning they cannot strictly be fit with 1:1 binding models – we elected to determine the siRNA-pAb kinetic constants to give a sense of what values

to expect for tight, specific, siRNA-protein interactions. By globally fitting the sensorgrams to a 1:1 model, we calculated an apparent K_D (~K_D) of 2.60 ± 0.03 nM, an apparent on rate (~k_{on}) of 3.661 x 10^4 ± 0.006 x 10^4 $M^{-1}.s^{-1}$, and an apparent off rate (~k_{off}) of 9.53 x 10^{-5} ± 0.09 x 10^{-5} s^{-1} (Fig. 5).

References

Gaus, H. J., R. Gupta, A. E. Chappell, M. E. Ostergaard, E. E. Swayze & P. P. Seth (2018) Characterization of the interactions of chemically-modified therapeutic nucleic acids with plasma proteins using a fluorescence polarization assay. *Nucleic Acids Res*.

Jankowsky, E. & M. E. Harris (2015) Specificity and nonspecificity in RNA-protein interactions. *Nat Rev Mol Cell Biol,* 16**,** 533-44.

Onishi, R., A. Watanabe, M. Nakajima, M. Sekiguchi, A. Kugimiya, H. Kinouchi, Y. Nihashi & H. Kamimori (2015) Surface Plasmon Resonance Assay of Binding Properties of Antisense Oligonucleotides to Serum Albumins and Lipoproteins. *Anal Sci,* 31**,** 1255-60.

Rustad, P., P. Felding, L. Franzson, V. Kairisto, A. Lahti, A. Martensson, P. Hyltoft Petersen, P. Simonsson, H. Steensland & A. Uldall (2004) The Nordic Reference Interval Project 2000: recommended reference intervals for 25 common biochemical properties. *Scand J Clin Lab Invest,* 64**,** 271-84.

Watanabe, T. A., R. S. Geary & A. A. Levin (2006) Plasma protein binding of an antisense oligonucleotide targeting human ICAM-1 (ISIS 2302). *Oligonucleotides,* 16**,** 169-80.